LINEAR HYDRODYNAMIC STABILITY OF FLUID FLOW IN CURVED RECTANGULAR DUCTS: SEMI-ANALYTICAL STUDY

H. Nowruzi

Department of Maritime Engineering,
Amirkabir University of Technology (Tehran Polytechnic)
Tehran, Iran

H. Ghassemi *

Department of Maritime Engineering,
Amirkabir University of Technology (Tehran Polytechnic)
Tehran, Iran

S. S. Nourazar

Department of Mechanical Engineering
Amirkabir University of Technology (Tehran Polytechnic)
Tehran, Iran

ABSTRACT

In the current study, for the first time, a semi-analytical technique is used for solving eigenvalue problem arising from linear hydrodynamics stability of fluid flow through the curved rectangular ducts at different curvature ratios and aspect ratios. To this accomplishment, symmetric disturbances are assumed and the Homotopy perturbation method (HPM) is applied to solve our eigenvalue problem for curvature ratios ranging from 0.01 to 0.8 and aspect ratios ranging from 0.05 to 20. Our semi-analytical results are validated through the existing numerical and experimental data, showing good agreement. The semi-analytical results indicate that, as the curvature ratio increases the critical Dean number (Dn_c) is increased and the flow becomes more stable, especially for aspect ratios lower than 1.Moreover, for all intended curvature ratios, irregular behavior in variation of Dn_c is detected by an increase in the aspect ratio. So that, the Dn_c is decreased when the aspect ratio increases from 0.05 up to 1 and the fluid flow becomes unstable. When the aspect ratio is increased from 1 to 5, it causes to increase the Dn_c and fluid flow becomes stable. Furthermore, when the aspect ratio increases from 5 to 20, the Dn_c is decreased again. In addition, Dn_c and eigenvalues of critical complex wave number corresponding to Dn_c for the onset of Dean flow instability is reported under different curvature ratios and aspect ratios.

Keywords: Hydrodynamic stability, Critical Dean number, Aspect ratio, Curvature ratio, Semi analytical method.

1. INTRODUCTION

Fluid flow through the non-circular curved ducts is a prevalent phenomenon in different macro and micro engineering fields. These ducts have an important application in macro system such as fluid machineries, turbines, turbo-compressor, cooling systems (i.e., heat exchangers and ventilators), entrance duct of water-jets systems, etc. In addition, these ducts are comprehensively used in micro and nano electromechanical systems (MEMS/NEMS) [1], in that lithographic method usually produce ducts with non-circular cross-section.

Inertial and centrifugal forces are governed in the fluid flow in the curved ducts. Subjected to centrifugal force, a counter-rotating vortex motion mounted on the axial flow are formed which is known as secondary flow [2]. Under the specific critical conditions, an imbalance between the pressure gradient and centrifugal forces in radial direction cause hydrodynamic instability and additional pairs of counter-rotating vortices (i.e., Dean Vortices) become evident in vicinity of the outer side of the curvature. The onset of instability is dependent on the Dean number (Dn) [2] as well as the geometrical parameters such as aspect ratio and curvature ratio of the curved ducts.

* Corresponding author (gasemi@aut.ac.ir)

DOI : 10.1017/jmech.2019.5
Copyright © 2019 The Society of Theoretical and Applied Mechanics

https://doi.org/10.1017/jmech.2019.5 Published online by Cambridge University Press

Nowadays, the problem of fluid flow stability in the curved ducts is considered as a classical issue in the field of linear hydrodynamics stability analysis. Therefore, fluid flow in the curved ducts is so far extensively studied by many researchers using numerical, experimental and semi-analytical methods. For example, fluid flow in rectangular curved duct and the symmetric and asymmetric steady solutions are studied by Winters [3] using finite element method (FEM). Chandratilleke and Nursubyakto [4] numerically carried out the secondary flow through curved rectangular ducts with aspect ratios of 1 to 8 under different Dean numbers ranging from 20 to 500. They showed that the aspect ratio is significantly impressive on the Dean vortices formation. They also reported the critical Dean numbers (Dn_{cs}) under different aspect ratios. The laminar flow in a curved rectangular duct over wide ranges of aspect ratios has been studied by Yanase *et al*. [5]. They studied the five branches of the steady solutions. Fellouah et al. [6] conducted a numerical study to investigate the laminar Dean flow stability in 180◦ curved duct under different curvature ratios and aspect ratios. They showed that Dean number is decreased as curvature ratio increases. The 3D developed secondary flows of Newtonian and visco-elastic fluids through a curved square duct using Phan-Thien-Tanner model simulated by Boutabaa *et al*. [7]. They found two and four cell patterns in the fluid domains under different Dean Numbers. Vinuesa *et al*. [8] studied the 3D effects of sidewall boundary layers and secondary motions in the turbulent duct flows using direct numerical simulation (DNS). They achieved a significant array of secondary vortices developing on the upper and lower walls of the duct which are effective by Reynolds number and aspect ratios. Recently, fluid flow behavior and heat transfer for peristalsis of MHD Carreau fluid in a curved channel in modified Darcy law investigated by Tanveer *et al*. [9].

Several other researches concerning the experimental method on fluid flow in curved ducts under different Dean number and geometrical characteristics have been conducted by Ligrani and Niver [10], Yamamoto *et al*. [11], and etc. For example, Sugiyama *et al*. [12] experimentally studied a fully developed laminar flow in the curved rectangular ducts with aspect ratios ranging from 0.5 to 2.5 and curvature ratios from 5 to 8. They indicated that the Dn_c has minimum and maximum values with respect to the aspect ratios of about 1 and 2.

From the viewpoint of semi-analytical and analytical studies on fluid flow in curved ducts, the pioneering study of the Dean [13] may be referred. He solved the equations of motion and continuity for incompressible viscous fluid flow between two parallel curved walls with small curvature, semi analytically. He also added infinite small disturbance to axisymmetric basic flow regardless of gravitational effects and axially periodic disturbance. Topakoglu [14] analytically investigated the fluid flow in curved circular pipes more comprehensively in comparison to Dean [13] study. He obtained an analytical solution for the pressure drop. Finlay and Nandakumar [15] analytically studied the Dean flow for larger aspect ratios. Walowit *et al*. [16] studied the stability of Dean flow via Galerkin method in conjunction with a simple set

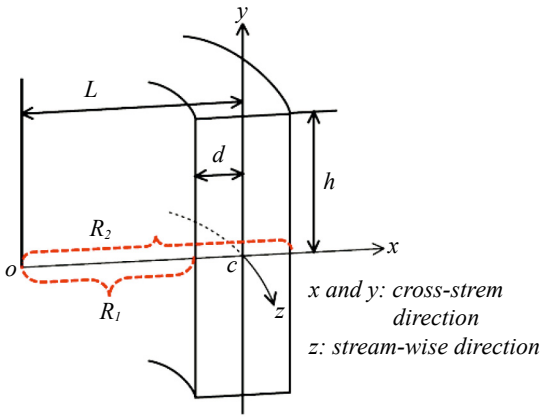


Fig. 1 Schematic of the problem

of polynomial expansion functions. Stability of Dean flow is also studied by Runge–Kutta scheme combined with a shooting method by Deka and Takhar [17]. Recently, Chen *et al*. [18] studied the fluid flow bifurcations in a rectangular curved duct under different aspect ratios and pressure gradients. They reported the range of stable flow and bifurcation points under different considered geometrical and physical conditions.

On the other hand, linear hydrodynamic stability method is one of the most effective approaches in field of fluid flow hydrodynamic stability analysis. In this method, calculation of spatially evolving modes is a main approach in analyzing linear hydrodynamic stability problem [1]. These modes are the function of wave number, in which the complex wave number is eigenvalue. This eigenvalue can be solved either numerically for example by using spectral method [19, 20, and 21] or semi-analytically like Deka and Paul [22] study in which Couette Taylor and Dean flow were solved using semi-analytical approach of differential transform method (DTM).

Along with the cited works, the evaluation of semi-analytical method for solving the characteristic value problems arising from linear hydrodynamic stability of fluid flow in the curved rectangular ducts is not so far studied. On the other hand, the effects of various curvature ratios under different aspect ratios are not well known to stabilize or destabilize the fluid flow through the curved ducts, especially under the wide range of the intended geometrical parameters. Thus, the main purpose of the current paper is to study the effects of different curvature ratios ranging from 0.01 to 0.8 and aspect ratios ranging from 0.05 to 20 on linear hydrodynamic stability of fluid flow through the curved ducts. For this purpose, linear hydrodynamic stability developed for symmetric disturbances of fully developed incompressible fluid flow in curved rectangular ducts is semi-analytically investigated via the Homotopy perturbation method (HPM) [23] as an efficient technique to obtain an approximate solution for eigenvalue problems..

2. GEOMETRY OF THE PROBLEM AND MATHEMATICAL MODEL

https://doi.org/10.1017/jmech.2019.5 Published online by Cambridge University Press

2.1. Basic equations

Consider the steady viscous and incompressible fluid flow through the curved rectangular duct as is illustrated in Fig.1. The rectangular coordinate system is shown that the x- and y-axes are cross-stream directions, the z-axis is stream-wise direction, and L is curvature radii.

According to Fig.1, the spatial X, Y, Z coordinates are non-dimensionalized by d, as in $x = X/d$, $y = Y/d$ and $z = Z/d$, also non-dimensionalized velocity are $u = U/w_{ref}$, $v = V/w_{ref}$ and $w = W/w_{ref}$ in x, y and z-directions (i.e., note that the z-axis is curved), respectively. Here, U, V and W are velocity with dimension and w_{ref} is a reference velocity. Curvature in each part of the duct is $1+\delta x$, where δ as curvature ratio is $\delta = D_h/L$ (i.e., where, D_h is hydraulic diameter as in $D_h = 4hd/(h+d)$). In the present study, the maximum velocity of fluid flow in a straight rectangular duct with the same hydraulic diameter and pressure gradient with considered curved duct is used as the reference velocity in form of $w_{ref} = G\,D_h^2/16\mu$ (where G and μ are constant gradient pressure in stream-wise direction and dynamic viscosity, respectively).

If the flow field along the duct in z-direction is assumed uniformity (i.e., rotationally symmetric), stream function may be used for sectional velocity components u and v. Moreover, due to axisymmetry flow through the considered curved duct (See Fig.1), Stokes stream function may be defined for sectional velocity components as follows (See more detail related to derivation of Stokes stream function in Ref. [24]):

$$\begin{cases} u = \dfrac{1}{r}\dfrac{\partial \psi}{\partial y} = \dfrac{1}{1+\delta x}\dfrac{\partial \psi}{\partial y} \\ v = -\dfrac{1}{r}\dfrac{\partial \psi}{\partial x} = -\dfrac{1}{1+\delta x}\dfrac{\partial \psi}{\partial x} \end{cases} \tag{1}$$

As may be seen in Eq.(1), r is the radial distance of each part of the duct from duct's center and according to Fig.1, r is equal to $1+\delta x$. In the present study, the y-coordinate is defined as $y = ly'$, where $l = h/d$ is the aspect ratio (continued for simplicity y' is shown by y).Under the condition of fully developed flow, derivations of fluid flow parameters in the stream-wise direction (along z-axis) are canceled except the static pressure. Definition of Stokes stream function in Eq.(1) satisfies the continuity equation and the basic equation for the stream-wise velocity (w) and ψ are derived from the Navier-Stokes equation as follows [5]:

$$\frac{1}{l}\frac{\partial(w,\psi)}{\partial(x,y)} = Dn - \frac{\delta^2 w}{(1+\delta x)} + (1+\delta x)\Delta_2 w - \frac{1}{l}\frac{\delta}{(1+\delta x)}\frac{\partial \psi}{\partial y}w + \delta\frac{\partial w}{\partial x}, \tag{2}$$

$$\begin{aligned} &-\frac{1}{l}\frac{1}{1+\delta x}\frac{\partial(\Delta_2\psi,\psi)}{\partial(x,y)} + \frac{1}{l}w\frac{\partial w}{\partial y} + \Delta_2^2\psi \\ &+\frac{1}{l}\frac{\delta}{(1+\delta x)^2}\left[\frac{\partial \psi}{\partial y}\left(2\Delta_2\psi - \frac{3\delta}{1+\delta x}\frac{\partial \psi}{\partial x} + \frac{\partial^2\psi}{\partial x^2}\right) - \frac{\partial \psi}{\partial x}\frac{\partial^2\psi}{\partial x \partial y}\right] \\ &+\frac{\delta}{(1+\delta x)^2}\left[-2(1+\delta x)\frac{\partial}{\partial x}\Delta_2\psi + 3\delta\frac{\partial^2\psi}{\partial x^2} - \frac{3\delta^2}{1+\delta x}\frac{\partial \psi}{\partial x}\right] = 0, \end{aligned} \tag{3}$$

where:

$$\begin{cases} \Delta_2 \equiv \dfrac{\partial^2}{\partial x^2} + \dfrac{1}{l^2}\dfrac{\partial^2}{\partial y^2}, \\ \dfrac{\partial(\mathrm{f},\mathrm{g})}{\partial(\mathrm{x},\mathrm{y})} \equiv \dfrac{\partial f}{\partial x}\dfrac{\partial g}{\partial y} - \dfrac{\partial f}{\partial y}\dfrac{\partial g}{\partial x}. \end{cases} \tag{4}$$

It is notable that, Eq.(2) is representative of momentum equation in the z-direction, while, Eq.(3) is presented for stream function equation that is achieved by incorporation of momentum equations in x and y- directions to eliminate the lateral pressure gradients. Dn is Dean number and the boundary conditions are given as follows:

https://doi.org/10.1017/jmech.2019.5 Published online by Cambridge University Press

$$w(\pm 1, y) = w(x, \pm 1) = \psi(\pm 1, y) = \frac{\partial \psi}{\partial x}(\pm 1, y) = \psi(x, \pm 1) = \frac{\partial \psi}{\partial y}(x, \pm 1) = 0. \tag{5}$$

In the present paper, only symmetrical steady solution is investigated. The reason of this selection is related to minor significant of asymmetric steady solution as reported by Winter [3], Yanase et al. [5] and Fellouah et al. [6], where all asymmetrical solutions in rectangular curved duct is linearly unstable. Moreover, as may be found in experimental studies [25-27], governing secondary flow on cross section of the rectangular curved ducts has symmetrical pattern along the horizontal mid-plane. So, based on the symmetrical fluid flow domain in y-direction, the symmetrical forms of boundary conditions in Eq.(5) are defined as follows:

$$w = \psi = \frac{\partial \psi}{\partial x} = 0 \quad @\, x = \pm 1 \tag{6}$$

$$\begin{cases} w = \psi = \dfrac{\partial \psi}{\partial y} = 0 \quad @\, y = 1 \\ \psi = \dfrac{\partial^2 \psi}{\partial y^2} = 0 \quad @\, y = 0 \end{cases} \tag{7}$$

2.2. Basic solution

If we assume the basic flow for this problem in form of uni-directional Dean flow as suggested by Drazin and Reid [2], the velocity distribution of basic flow becomes independent from cross-stream velocity components of u and v. This assumption is corresponding to stream-function $\psi = 0$ (See Eq.(1)). According to this assumption and by integration of reduced form Eq.(2) and using the boundary conditions Eqs.(6) and (7), the basic stream-wise velocity distribution in familiar form of Poiseuille flow may be defined as follows:

$$w(x) = A(xd + L) + \frac{B}{(xd + L)} + M(xd + L)\ln(xd + L) \tag{8}$$

here, $M = \frac{1}{2\rho\upsilon}\left(\frac{\partial p}{\partial \theta}\right)_0$ where, ρ , υ and $\left(\frac{\partial p}{\partial \theta}\right)_0$ are density, kinematic viscosity and constant azimuthal pressure gradient, respectively. Moreover, the constant of A and B are achieved as follows:

$$\begin{cases} A = \dfrac{M\left(\ln R_2 - \left(\dfrac{R_1}{R_2}\right)^2 \ln R_1\right)}{\left(\dfrac{R_1}{R_2}\right)^2 - 1}, \\ B = \dfrac{M\left(R_1^2 \ln \dfrac{R_1}{R_2}\right)}{\left(\dfrac{R_1}{R_2}\right)^2 - 1}, \end{cases} \tag{9}$$

Dean number (Dn) may be defined as [28]:

$$Dn = \mathrm{Re}\left(D_h / L\right)^{0.5} \tag{10}$$

where, Re is Reynolds number as follows:

$$\mathrm{Re} = \frac{w_m (D_h)}{\upsilon} \tag{11}$$

https://doi.org/10.1017/jmech.2019.5 Published online by Cambridge University Press

here, w_m as an average velocity is:

$$w_m = \frac{1}{R_2 - R_1}\int_{R_1}^{R_2} V(r)dr = \frac{MR_2}{4\left(1-\frac{R_1}{R_2}\right)}\left[\frac{\left(\left(\frac{R_1}{R_2}\right)^2 - 1\right)^2 - \left(2\frac{R_1}{R_2}\ln\frac{R_1}{R_2}\right)^2}{\left(\frac{R_1}{R_2}\right)^2 - 1}\right] \tag{12}$$

2.3. Linear hydrodynamic stability

According to the basic state of fluid flow in curved duct, we impose infinitesimally small disturbances on it and then trace the process of how it responds to such disturbances in order to analyze the linear hydrodynamic stability. Small disturbances of ψ' and w' are imposed on basic solution $\overline{\psi}$ and $\overline{w}$ as $\overline{\psi}+\psi'$ and $\overline{w}+w'$ .These disturbances are applied to the Eqs. (2) and (3). After some mathematical manipulations, linear stability analysis for the fluid flow in rectangular curved duct is defined as:

$$\begin{aligned}
&(1+\delta x)\Delta w' + \delta\frac{\partial w'}{\partial x} - \frac{\delta^2 w'}{1+\delta x} \\
&-\frac{1}{l}\frac{\partial(\overline{w},\psi')}{\partial(x,y)} - \frac{1}{l}\frac{\partial(w',\overline{\psi})}{\partial(x,y)} - \frac{1}{l}\frac{\delta}{1+\delta x}\frac{\partial\psi'}{\partial y}\overline{w} - \frac{1}{l}\frac{\delta}{(1+\delta x)}\frac{\partial\overline{\psi}}{\partial y}w' = 0,
\end{aligned} \tag{13}$$

$$\begin{aligned}
&-\frac{2\delta}{1+\delta x}\frac{\partial}{\partial x}\Delta\psi' + \frac{\delta^2}{(1+\delta x)^2}\Delta\psi' \\
&-\frac{\delta^2}{l^2(1+\delta x)^2}\frac{\partial^2\psi'}{\partial y^2} + \frac{2\delta^2}{(1+\delta x)^2}\frac{\partial^2\psi'}{\partial x^2} - \frac{3\delta^3}{(1+\delta x)^3}\frac{\partial\psi'}{\partial x} + \Delta^2\psi' \\
&-\frac{1}{l}\frac{1}{1+\delta x}\frac{\partial(\Delta\overline{\psi},\psi')}{\partial(x,y)} - \frac{1}{l}\frac{1}{1+\delta x}\frac{\partial(\Delta\psi',\overline{\psi})}{\partial(x,y)} \\
&+\frac{1}{l}\frac{\partial\overline{\psi}}{\partial y}\left\{\frac{2\delta}{(1+\delta x)^2}\Delta\psi' - \frac{3\delta^2}{(1+\delta x)^3}\frac{\partial\psi'}{\partial x} + \frac{\delta}{(1+\delta x)^2}\frac{\partial^2\psi'}{\partial x^2}\right\} \\
&+\frac{1}{l}\frac{\partial\psi'}{\partial y}\left\{\frac{2\delta}{(1+\delta x)^2}\Delta\overline{\psi} - \frac{3\delta^2}{(1+\delta x)^3}\frac{\partial\overline{\psi}}{\partial x} + \frac{\delta}{(1+\delta x)^2}\frac{\partial^2\overline{\psi}}{\partial x^2}\right\} \\
&-\frac{1}{l}\frac{\delta}{(1+\delta x)^2}\frac{\partial\overline{\psi}}{\partial x}\frac{\partial^2\psi'}{\partial x\partial y} - \frac{1}{l}\frac{\delta}{(1+\delta x)^2}\frac{\partial\psi'}{\partial x}\frac{\partial^2\overline{\psi}}{\partial x\partial y} + \frac{1}{l}\overline{w}\frac{\partial w'}{\partial y} + \frac{1}{l}w'\frac{\partial\overline{w}}{\partial y} = 0,
\end{aligned} \tag{14}$$

The boundary conditions for small disturbances are:

$$\begin{aligned}
&w'(\pm1,y) = \psi'(\pm1,y) = \frac{\partial\psi'}{\partial x}(\pm1,y) = 0 \\
&w'(\mathrm{x},+1) = \psi'(\mathrm{x},+1) = \frac{\partial\psi'}{\partial y}(\mathrm{x},+1) = 0 \\
&\psi'(\mathrm{x},0) = \frac{\partial^2\psi'}{\partial y^2}(x,0) = 0.
\end{aligned} \tag{15}$$

According to the concept of normal modes, the disturbed parameters for the stream function and steam-wise velocity may be defined as:

$$\begin{cases}
\psi(x,y,\mathrm{t}) = \overline{\psi} + \psi' = \overline{\psi} + \hat{\psi}(x)e^{iky+\sigma t} \\
w(x,y,\mathrm{t}) = \overline{w} + w' = \overline{w} + \hat{w}(x)e^{iky+\sigma t}
\end{cases} \tag{16}$$

https://doi.org/10.1017/jmech.2019.5 Published online by Cambridge University Press

where the over bar (-) is basic flow, the prime (') shows the disturbances, and the hat (^) symbol indicates the amplitude of disturbances. In addition, K and σ are wave number and amplification or growth rate (frequency), respectively. Thus, Eqs. (13) and (14) can be redefined by the linearized disturbance equations for the linear hydrodynamic stability of fluid flow in curved rectangular duct as:

$$
\begin{aligned}
&(1+\delta x)\left(\sigma\hat{w}(x)\right) = (1+\delta x)\left[\left(D_{2x}\hat{w}(x)\right) - \frac{k^2}{l^2}\hat{w}(x)\right] + \delta\left[D_x\hat{w}(x)\right] \\
&-\frac{\delta^2\hat{w}(x)}{1+\delta x} - \frac{1}{l}\left[ik\left(D_x\bar{w}\right)\hat{\psi}(x) - \left(\left(D_y\bar{w}\right)\left(D_x\hat{\psi}(x)\right)\right)\right] \\
&-\frac{1}{l}\left[\left(\left(D_x\hat{w}(x)\right)\left(D_y\bar{\psi}\right)\right) - \left(\hat{w}(x)ik\left(D_x\bar{\psi}\right)\right)\right] - \frac{1}{l}\frac{\delta}{1+\delta x}\hat{\psi}(x)ik\bar{w} - \frac{1}{l}\frac{\delta}{(1+\delta x)}\left[D_y\bar{\psi}\right]\hat{w}(x),
\end{aligned}
\tag{17}
$$

$$
\begin{aligned}
&\left[\left(D_{2x}\hat{\psi}(x)\sigma\right) - \left(\frac{k^2}{l^2}\sigma\hat{\psi}(x)\right)\right] - \left(\frac{\delta}{(1+\delta x)}\sigma\left(D_x\hat{\psi}(x)\right)\right) = -\frac{2\delta}{(1+\delta x)}\left[\left(D_{3x}\hat{\psi}(x)\right) - \left(\frac{k^2}{l^2}\left(D_x\hat{\psi}(x)\right)\right)\right] \\
&+\frac{\delta^2}{(1+\delta x)^2}\left[\left(D_{2x}\hat{\psi}(x)\right) - \left(\frac{k^2}{l^2}\hat{\psi}(x)\right)\right] - \frac{\delta^2}{l^2(1+\delta x)^2}\left[-k^2\hat{\psi}(x)\right] + \frac{2\delta^2}{(1+\delta x)^2}\left[\left(D_{2x}\hat{\psi}(x)\right)\right] \\
&-\frac{3\delta^3}{(1+\delta x)^3}\left[\left(D_x\hat{\psi}(x)\right)\right] + \left(\left[D_{4x}\hat{\psi}(x)\right] - \frac{2k^2}{l^2}\left(D_{2x}\hat{\psi}(x)\right) + \frac{k^4}{l^4}\hat{\psi}(x)\right) \\
&-\frac{1}{l}\frac{1}{(1+\delta x)}\left[\left(\left(D_{3x}\bar{\psi}\right) + \frac{1}{l^2}D_xD_{2y}\bar{\psi}\right)\left(ik\hat{\psi}(x)\right) - \left(D_yD_{2x}\bar{\psi} + \frac{1}{l^2}D_{3y}\bar{\psi}\right)\left(D_x\hat{\psi}(x)\right)\right] \\
&-\frac{1}{l}\frac{1}{(1+\delta x)}\left[\left(\left(D_{3x}\hat{\psi}(x)\right) - \frac{k^2}{l^2}\left(D_x\hat{\psi}(x)\right)\right)\left(D_y\bar{\psi}\right) - \left(ik\left(D_{2x}\hat{\psi}(x)\right) - \frac{ik^3}{l^2}\hat{\psi}(x)\right)\left(D_x\bar{\psi}\right)\right] \\
&+\frac{1}{l}\left[D_y\bar{\psi}\right]\left\{\left(\frac{2\delta}{(1+\delta x)^2}\left(\left(D_{2x}\hat{\psi}(x)\right) - \frac{k^2}{l^2}\hat{\psi}(x)\right)\right) - \left(\frac{3\delta^2}{(1+\delta x)^3}\left(D_x\hat{\psi}(x)\right)\right) + \left(\frac{\delta}{(1+\delta x)^2}\left(D_{2x}\hat{\psi}(x)\right)\right)\right\} \\
&+\frac{ik}{l}\hat{\psi}(x)\left\{\left(\frac{2\delta}{(1+\delta x)^2}\left(\left(D_{2x}\bar{\psi}\right) + \frac{1}{l^2}\left(D_{2y}\bar{\psi}\right)\right)\right) - \left(\frac{3\delta^2}{(1+\delta x)^3}\left(D_x\bar{\psi}\right)\right) + \left(\frac{\delta}{(1+\delta x)^2}\left(D_{2x}\bar{\psi}\right)\right)\right\} \\
&-\left(\frac{1}{l}\frac{\delta}{(1+\delta x)^2}\left(D_x\bar{\psi}\right)\left(ik\left(D_x\hat{\psi}(x)\right)\right)\right) - \left(\frac{1}{l}\frac{\delta}{(1+\delta x)^2}\left(D_x\hat{\psi}(x)\right)\left(D_xD_y\bar{\psi}\right)\right) \\
&+\left(\frac{1}{l}\bar{w}\left(ik\hat{w}(x)\right)\right) + \left(\frac{1}{l}\hat{w}(x)\left(D_y\bar{w}\right)\right).
\end{aligned}
\tag{18}
$$

where;

$$
\begin{cases}
D_x = \dfrac{d}{dx} & D_y = \dfrac{d}{dy} & D_{2x} = \dfrac{d^2}{dx^2} \\
D_{2y} = \dfrac{d^2}{dy^2} & D_{3x} = \dfrac{d^3}{dx^3} & D_{3y} = \dfrac{d^3}{dy^3} \\
D_{4x} = \dfrac{d^4}{dx^4} & D_{4y} = \dfrac{d^4}{dy^4} & D_xD_y = \dfrac{d}{dx}\left(\dfrac{d}{dy}\right)
\end{cases}
\tag{19}
$$

For flow in the curved ducts, the onset of instability is steady secondary motion, so marginal state is stationary ($\sigma = 0$). In the present study, disturbances are assumed symmetrical about the y-axis and therefore, they are independent from z and dependent on x, y. Indeed, stability of motion is dependent on the exponential temporal factor of $\sigma = \sigma_r + i\sigma_i$. In case of real part of $\sigma_r > 0$, the motion is unstable and it is stable for $\sigma_r < 0$. As a result, the marginal state (i.e., neutral stability) is determined by $\sigma_r = 0$. Under the condition of neutral

https://doi.org/10.1017/jmech.2019.5 Published online by Cambridge University Press

stability, if $\sigma_i \neq 0$, we have over stability (i.e., purely oscillatory motion) condition; also a stationary cellular motion is detectable in case of $\sigma_i = 0$. Accordingly, in the present problem, instability has spatial form and we analyze the marginal state (i.e., $\sigma = 0$) [16]. In case of $\sigma = \sigma_r + i\sigma_i = fixed = 0$ (i.e., neutral stable condition), complex value of wave number $k = k_r + ik_i$ should be analyzed. Since the real part of wave number is positive $k_r > 0$, in spatial stability analysis, the imaginary part of the wave number is examined. So that, in case of $k_i > 0$, we have linearly stable condition which represents the decay of disturbances, while $k_i < 0$ is a linearly unstable condition that is related to amplification of disturbances. In addition, $k_i = 0$ is a neutral stable condition [2]. Indeed, to proceed with this study, we capture the first mode of instability (i.e., stationary mode) before bifurcation of the solutions. It is also notable that, in the framework of the eigenvalue approach arising from linear hydrodynamic stability, there is no absolute means to predict which formulation (e.g. temporal or spatial) corresponds to a considered problem in a given reference system. Therefore, for identifying how the small disturbance is developed, it is necessary to focus on the impulse response of the intended system.

In other words, as shown by scholars [26, 29, 30], the hydrodynamic instability in curved ducts is convective instability, where the state of convectively unstable fluid flow is identified by small disturbances which are selectively amplified in the direction of fluid motion (i.e., imposed disturbances will be convected down-stream as they develop in some way [31]). Therefore, according to the cited works [26, 29, 30, 31] and Huerre and Monkewitz [27] study, as the nature of instability in fluid flow through the curved duct is convective, the spatial stability analysis is appropriate to investigate the hydrodynamic stability in curved ducts. Meantime, it is recognizable from lab experiments that small-amplitude disturbances amplify downstream in many open near-wall shear layers such as flows in channel, (i.e., Dean flow in curved duct) at least at the Dean numbers which are practically significant. Therefore, one may assume even without theoretical justification that it is more appropriate for such basic flows to consider the spatial stability. Indeed, we may consider the small disturbance waves with real frequencies σ (i.e., for Dean flow in curved duct σ=0) and complex wave numbers k. In mathematical studies of spatial instability, the Dean number and the disturbance frequency σ are given, while k will be calculated by solving the eigenvalue equation.

Moreover, the semi-analytical method of HPM is evaluated for solving the eigenvalue problem expressed by Eqs. (17) and (18). Generally, in solution procedure, we obtain matrix of linear homogenous equations using Eqs. (17) and (18) and by satisfying the boundary condition. To achieve the non-trivial solution, determinant of this matrix must vanish. By putting the determinate of matrix equal to zero, we determine a characteristic equation in terms of the unknowns k according to considered Dean number (Dn), curvature ratio (δ) and aspect ratio (l).

3. SOLUTION OF THE PROBLEM BY HPM

3.1. Basic concept of HPM

Here, we review the fundamental concepts of HPM for the convenience to the reader. Consider a nonlinear differential equation as follows:

$$L(v) + \mathrm{N}(v) - g(r) = 0 \quad r \in \Omega \tag{20}$$

Subjected to the boundary condition

$$B(v, \partial v/\partial n) = 0 \quad r \in \Gamma \tag{21}$$

where, L is a linear differential operator, N is a non-linear differential operator and $g(r)$ is an analytical function. Boundary operator is demonstrated by B , Γ is a boundary domain Ω and $\partial v/\partial n$ is a differentiation along the normal drawn outwards from Ω . The Homotopy on Eq.(20) may be applied as follows:

$$H(u, p) = L(\mathrm{u}) - L(v_0) + pL(v_0) + p(\mathrm{N}(u) - g(r)) = 0 \tag{22}$$

where

$$u(r, p) : \Omega \times [0,1] \to R, \tag{23}$$

https://doi.org/10.1017/jmech.2019.5 Published online by Cambridge University Press

here, the first approximation which satisfies the boundary condition is shown by v_0 while $p \in [0,1]$ is an embedding parameter. The solution of Eq.(22) as a form of power series in p , is written as follows:

$$u = u_0 + pu_1 + p^2 u_2 + \ldots \tag{24}$$

In this condition, approximated solution is

$$v = \lim_{m \to 1} u = u_0 + u_1 + u_2 + \ldots \tag{25}$$

3.2. Solution by HPM

Let's assume the $\hat{\psi}(x) \to f(x)$ and $\hat{w}(x) \to g(x)$ in Eqs. (17) and (18), then we have;

$$\begin{aligned}
&\left[(D_{2x} g(x)) - \frac{k^2}{l^2} g(x) \right] + \frac{\delta}{(1+\delta x)} [D_x g(x)] \\
&- \frac{\delta^2 g(x)}{(1+\delta x)^2} - \frac{1}{l(1+\delta x)} \left[ik \left(Ad - \frac{Bd}{(xd+L)^2} + M(d + d\ln(xd+L)) \right) f(x) \right] \\
&- \frac{\delta}{l(1+\delta x)^2} f(x) ik \left(A(xd+L) + \frac{B}{(xd+L)} + M(xd+L)\ln(xd+L) \right) = 0,
\end{aligned} \tag{26}$$

$$\begin{aligned}
&- \frac{2\delta}{(1+\delta x)} \left[(D_{3x} f(x)) - \left(\frac{k^2}{l^2} (D_x f(x)) \right) \right] \\
&+ \frac{\delta^2}{(1+\delta x)^2} \left[(D_{2x} f(x)) - \left(\frac{k^2}{l^2} f(x) \right) \right] - \frac{\delta^2}{l^2 (1+\delta x)^2} [-k^2 f(x)] + \frac{2\delta^2}{(1+\delta x)^2} [(D_{2x} f(x))] \\
&- \frac{3\delta^3}{(1+\delta x)^3} [(D_x f(x))] + \left([D_{4x} f(x)] - \frac{2k^2}{l^2} (D_{2x} f(x)) + \frac{k^4}{l^4} f(x) \right) \\
&+ \left(\frac{1}{l} \left(A(xd+L) + \frac{B}{(xd+L)} + M(xd+L)\ln(xd+L) \right) (ikg(x)) \right) = 0.
\end{aligned} \tag{27}$$

The boundary conditions will also have the following form:

$$\begin{aligned}
&g(+1) = 0 \quad ; \quad g(-1) = 0 \\
&f(+1) = 0 \quad ; \quad f(-1) = 0 \quad ; \quad D_x f(+1) = 0 \quad ; \quad D_x f(-1) = 0
\end{aligned} \tag{28}$$

here, HPM is applied to Eqs. (26) and (27). Based on HPM, the Eqs. (26) and (27) are conducted as follows:

$$\begin{aligned}
&H_1(g,p) = (1-p)[(D_{2x} g) - (D_{2x} g_0)] \\
&+ p \left(\begin{aligned}
&\left[(D_{2x} g(x)) - \frac{k^2}{l^2} g(x) \right] + \frac{\delta}{(1+\delta x)} [D_x g(x)] \\
&- \frac{\delta^2 g(x)}{(1+\delta x)^2} - \frac{1}{l(1+\delta x)} \left[ik \left(Ad - \frac{Bd}{(xd+L)^2} + M(d + d\ln(xd+L)) \right) f(x) \right] \\
&- \frac{\delta}{l(1+\delta x)^2} f(x) ik \left(A(xd+L) + \frac{B}{(xd+L)} + M(xd+L)\ln(xd+L) \right)
\end{aligned} \right) = 0
\end{aligned} \tag{29}$$

https://doi.org/10.1017/jmech.2019.5 Published online by Cambridge University Press

$$H_2(f,p)=(1-p)\left((D_{4x}f)-(D_{4x}f_0)\right)$$
$$+p\left(\begin{array}{l}-\dfrac{2\delta}{(1+\delta x)}\left[(D_{3x}f(x))-\left(\dfrac{k^2}{l^2}(D_xf(x))\right)\right]\\+\dfrac{\delta^2}{(1+\delta x)^2}\left[(D_{2x}f(x))-\left(\dfrac{k^2}{l^2}f(x)\right)\right]-\dfrac{\delta^2}{l^2(1+\delta x)^2}\left[-k^2f(x)\right]+\dfrac{2\delta^2}{(1+\delta x)^2}\left[(D_{2x}f(x))\right]\\-\dfrac{3\delta^3}{(1+\delta x)^3}\left[(D_xf(x))\right]+\left(\left[D_{4x}f(x)\right]-\dfrac{2k^2}{l^2}(D_{2x}f(x))+\dfrac{k^4}{l^4}f(x)\right)\\+\left(\dfrac{1}{l}\left(A(xd+L)+\dfrac{B}{(xd+L)}+M(xd+L)\ln(xd+L)\right)(ikg(x))\right)\end{array}\right)=0 \tag{30}$$

Now, we define the general solutions as power series:

$$\begin{cases}f=f_0+pf_1+p^2f_2+p^3f_3+\ldots\\g=g_0+pg_1+p^2g_2+p^3g_3+\ldots\end{cases} \tag{31}$$

Let us assume the f_0 and g_0 are defined in which to satisfy the boundary conditions in Eq.(28) as follows:

$$\begin{cases}f_0=D_1\left(x^3-3x-2\right)+D_2\left(x^2+2x+1\right)\\g_0=D_3\left(x+1\right)\end{cases} \tag{32}$$

By substituting f and g from Eq. (31) into Eqs. (29) and (30) and assuming $D_{4x}f_0=0$ and $D_{2x}g_0=0$, we have:
For first Eq. (29):

$$p^0:\quad \{D_{2x}g_0=0 \tag{33}$$

$$p^1:\quad\left\{\begin{array}{l}D_{2x}g_1-\dfrac{k^2}{l^2}g_0+\dfrac{\delta}{(1+\delta x)}(D_xg_0)\\-\dfrac{\delta^2g_0}{(1+\delta x)^2}-\dfrac{1}{l(1+\delta x)}\left[ik\left(Ad-\dfrac{Bd}{(xd+L)^2}+M\left(d+d\ln(xd+L)\right)\right)f_0\right]\\-\dfrac{\delta}{l(1+\delta x)^2}f_0ik\left(A(xd+L)+\dfrac{B}{(xd+L)}+M(xd+L)\ln(xd+L)\right)=0\end{array}\right.$$

$$p^2:\quad\left\{\begin{array}{l}D_{2x}g_2-\dfrac{k^2}{l^2}g_1+\dfrac{\delta}{(1+\delta x)}(D_xg_1)\\-\dfrac{\delta^2g_1}{(1+\delta x)^2}-\dfrac{1}{l(1+\delta x)}\left[ik\left(Ad-\dfrac{Bd}{(xd+L)^2}+M\left(d+d\ln(xd+L)\right)\right)f_1\right]\\-\dfrac{\delta}{l(1+\delta x)^2}f_1ik\left(A(xd+L)+\dfrac{B}{(xd+L)}+M(xd+L)\ln(xd+L)\right)=0\end{array}\right.$$

https://doi.org/10.1017/jmech.2019.5 Published online by Cambridge University Press

$$p^3:\quad \begin{cases} D_{2x}g_3-\dfrac{k^2}{l^2}g_2+\dfrac{\delta}{(1+\delta x)}\left(D_x g_2\right) \\ -\dfrac{\delta^2 g_2}{(1+\delta x)^2}-\dfrac{1}{l(1+\delta x)}\left[ik\left(Ad-\dfrac{Bd}{(xd+L)^2}+M\left(d+d\ln\left(xd+L\right)\right)\right)f_2\right] \\ -\dfrac{\delta}{l(1+\delta x)^2}f_2 ik\left(A(xd+L)+\dfrac{B}{(xd+L)}+M\left(xd+L\right)\ln\left(xd+L\right)\right)=0 \end{cases}$$

$\vdots$

For second Eq. (30):

$$p^0:\quad \{D_{4x}f_0=0 \tag{34}$$

$$p^1:\quad \begin{cases} D_{4x}f_1-\dfrac{2k^2}{l^2}\left(D_{2x}f_0\right)+\dfrac{k^4}{l^4}f_0-\dfrac{2\delta}{(1+\delta x)}\left[\left(D_{3x}f_0\right)-\left(\dfrac{k^2}{l^2}\left(D_x f_0\right)\right)\right] \\ +\dfrac{\delta^2}{(1+\delta x)^2}\left[\left(D_{2x}f_0\right)-\left(\dfrac{k^2}{l^2}f_0\right)\right]-\dfrac{\delta^2}{l^2(1+\delta x)^2}\left[-k^2 f_0\right]+\dfrac{2\delta^2}{(1+\delta x)^2}\left[\left(D_{2x}f_0\right)\right] \\ -\dfrac{3\delta^3}{(1+\delta x)^3}\left[\left(D_x f_0\right)\right]+\left(\dfrac{1}{l}\left(A(xd+L)+\dfrac{B}{(xd+L)}+M\left(xd+L\right)\ln\left(xd+L\right)\right)\left(ikg_0\right)\right)=0 \end{cases}$$

$$p^2:\quad \begin{cases} D_{4x}f_2-\dfrac{2k^2}{l^2}\left(D_{2x}f_1\right)+\dfrac{k^4}{l^4}f_1-\dfrac{2\delta}{(1+\delta x)}\left[\left(D_{3x}f_1\right)-\left(\dfrac{k^2}{l^2}\left(D_x f_1\right)\right)\right] \\ +\dfrac{\delta^2}{(1+\delta x)^2}\left[\left(D_{2x}f_1\right)-\left(\dfrac{k^2}{l^2}f_1\right)\right]-\dfrac{\delta^2}{l^2(1+\delta x)^2}\left[-k^2 f_1\right]+\dfrac{2\delta^2}{(1+\delta x)^2}\left[\left(D_{2x}f_1\right)\right] \\ -\dfrac{3\delta^3}{(1+\delta x)^3}\left[\left(D_x f_1\right)\right]+\left(\dfrac{1}{l}\left(A(xd+L)+\dfrac{B}{(xd+L)}+M\left(xd+L\right)\ln\left(xd+L\right)\right)\left(ikg_1\right)\right)=0 \end{cases}$$

$$p^3:\quad \begin{cases} D_{4x}f_3-\dfrac{2k^2}{l^2}\left(D_{2x}f_2\right)+\dfrac{k^4}{l^4}f_2-\dfrac{2\delta}{(1+\delta x)}\left[\left(D_{3x}f_2\right)-\left(\dfrac{k^2}{l^2}\left(D_x f_2\right)\right)\right] \\ +\dfrac{\delta^2}{(1+\delta x)^2}\left[\left(D_{2x}f_2\right)-\left(\dfrac{k^2}{l^2}f_2\right)\right]-\dfrac{\delta^2}{l^2(1+\delta x)^2}\left[-k^2 f_2\right]+\dfrac{2\delta^2}{(1+\delta x)^2}\left[\left(D_{2x}f_2\right)\right] \\ -\dfrac{3\delta^3}{(1+\delta x)^3}\left[\left(D_x f_2\right)\right]+\left(\dfrac{1}{l}\left(A(xd+L)+\dfrac{B}{(xd+L)}+M\left(xd+L\right)\ln\left(xd+L\right)\right)\left(ikg_2\right)\right)=0 \end{cases}$$

$\vdots$

General closed form solution of differential equations (Eqs. (33) and (34)) as initial value problem are obtained via symbolic technique by using Maple software package [32]. Then, the general solution will be subjected to the boundary conditions given in Eq. (28) for finding the solution for k which is the eigenvalue of the problem at the specified constant value of $\sigma=0$. This procedure will lead to homogeneous linear equations, where determinant is set to zero and algebraic equation will be provided for determination of eigenvalue k according to considered Dean number (Dn), curvature ratio (δ) and aspect ratio (l). In the following, the effects of different curvature ratios and aspect ratios on the onset of Dean instability is investigated.

4. RESULTS AND DISCUSSION

4.1. Special case (i.e. Dean flow)

To confirm the present semi-analytical method, in case of Dean approximation as $L \gg D_h$ and *l=1*, by solving the characteristics value problem and determining principal (minimum) eigenvalue, critical values of Dean number (Dn_c) is achieved. The values of Dn_c obtained by HPM is compared with numerical solution. Spectral method is used for numerical solution of Eqs. (26) and (27) subjected to boundary conditions given in Eq.(28). For

https://doi.org/10.1017/jmech.2019.5 Published online by Cambridge University Press

Table 1Eigenvalue parameter, Dn_c, calculated by HPM at several k under different N compared to numerical solution.

k	HPM at several N				Numerical solution	Error (%) N=10	Error (%) N=15
	N=3	N=7	N=10	N=15			
1	83.90006267	84.26508431	84.26569937	84.26577560	84.26577614	9.11E-05	6.36E-07
3	38.99188851	38.68604743	38.68260276	38.68243031	38.68242908	4.49E-04	3.18E-06
6	37.20006713	36.68549856	36.69854903	36.69984629	36.69984820	3.54E-03	5.21E-06
10	43.57502767	46.08751976	46.02972968	46.03319608	46.03320058	7.54E-03	9.77E-06

Table 2 Values of $Dn_{c,\min}$ and corresponding k from HPM ($N=15$) compared to archival data.

Method of solution		k	Dn_c
Present study	HPM (N=15)	3.952	35.927
Archival data	Fourier expansion [2]	3.954	35.95
	Galerkin method [16]	3.96	35.90
	Runge–Kutta Fehlberg method [17]	3.96	35.922
	Differential transform method[22]	3.950	35.922

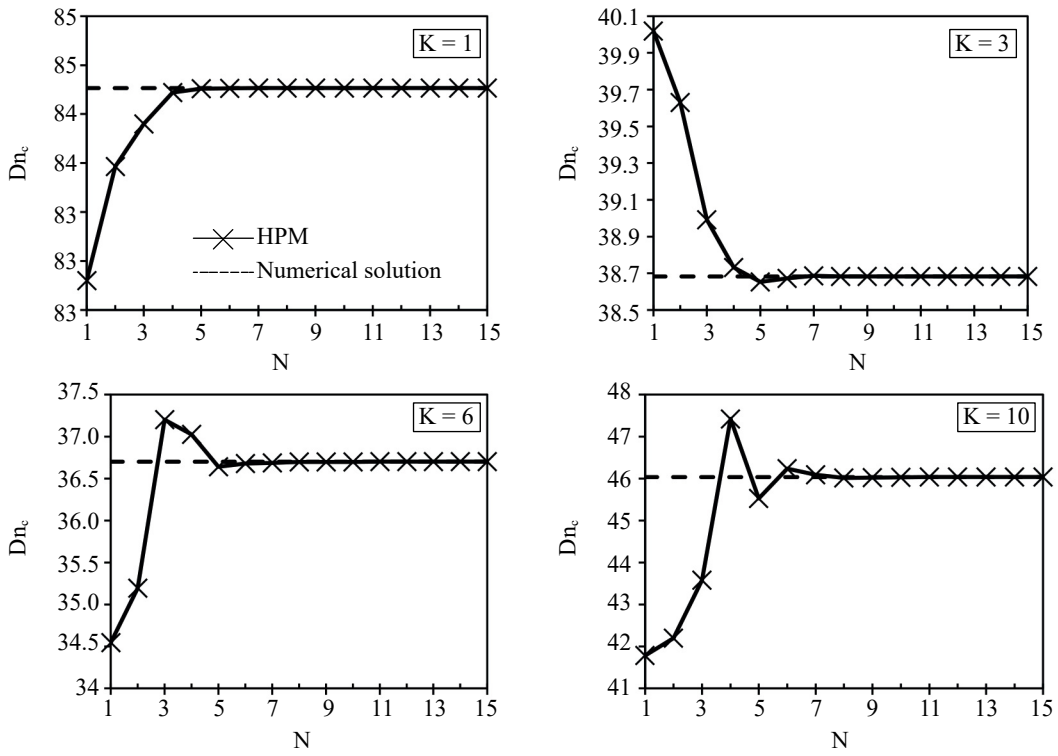


Fig. 2 Eigenvalue parameter, Dn_c, obtained by HPM at several k under different N

this purpose, all variables are expanded as a sum of certain trial functions. In the current study, the Chebyshev polynomial is used [19]. We used 120 truncation terms which are high enough to assure the accuracy of the numerical solution [5].

Dn_c is calculated by using HPM for several k (i.e. real constant wave number) and N (i.e. number of truncated terms), and the results are shown in Fig. 2. As observed, the results are in good agreement between numerical solutions and HPM for all intended wave numbers. According to Fig. 2, for $1 \le k \le 10$, the convergence is attained at $N=9$ for HPM. Table 1 is also given the percentage of relative error of the semi-analytical method and numerical solution.

According to literature studies dealing with linear stability analysis [2, 16, 17, 22], the criteria for onset of instability is the minimum of Dn_{cs} ($Dn_{c,\min}$) and its corresponding value of k. Hence, Dn_{cs} under different k obtained by HPM (N=15) is depicted in Fig. 3. Number of

https://doi.org/10.1017/jmech.2019.5 Published online by Cambridge University Press

Table 3 Considered test cases for parametric study on linear hydrodynamic stability of fluid flow through the curved duct under different δ and l and number of truncated terms used in HPM.

Curvature ratio	Aspect ratio	Geometrical parameters (See Fig.1)			Number of truncated terms used in HPM
$(\delta = D_h / L)$	$(l = h/d)$	L	h	d	N
0.01	0.05	19.048	0.05	1	16
	0.1	36.364	0.1	1	17
	0.5	133.333	0.5	1	17
	1	200	1	1	18
	5	333.333	5	1	17
	10	363.636	10	1	17
	20	380.952	20	1	16
0.05	0.05	3.810	0.05	1	17
	0.1	7.273	0.1	1	18
	0.5	26.667	0.5	1	17
	1	40	1	1	19
	5	66.667	5	1	17
	10	72.727	10	1	18
	20	76.190	20	1	18
0.1	0.05	1.905	0.05	1	18
	0.1	3.636	0.1	1	18
	0.5	13.333	0.5	1	19
	1	20	1	1	19
	5	33.333	5	1	19
	10	36.364	10	1	18
	20	38.095	20	1	18
0.2	0.05	0.952	0.05	1	19
	0.1	1.818	0.1	1	19
	0.5	6.667	0.5	1	18
	1	10	1	1	20
	5	16.667	5	1	18
	10	18.182	10	1	19
	20	19.048	20	1	19
0.4	0.05	0.476	0.05	1	20
	0.1	0.909	0.1	1	20
	0.5	3.333	0.5	1	19
	1	5	1	1	21
	5	8.333	5	1	19
	10	9.091	10	1	20
	20	9.524	20	1	20
0.6	0.05	0.317	0.05	1	21
	0.1	0.606	0.1	1	20
	0.5	2.222	0.5	1	22
	1	3.333	1	1	22
	5	5.556	5	1	22
	10	6.061	10	1	20
	20	6.349	20	1	21
0.8	0.05	0.238	0.05	1	21
	0.1	0.455	0.1	1	21
	0.5	1.667	0.5	1	22
	1	2.5	1	1	23
	5	4.167	5	1	22
	10	4.545	10	1	21
	20	4.762	20	1	21

https://doi.org/10.1017/jmech.2019.5 Published online by Cambridge University Press

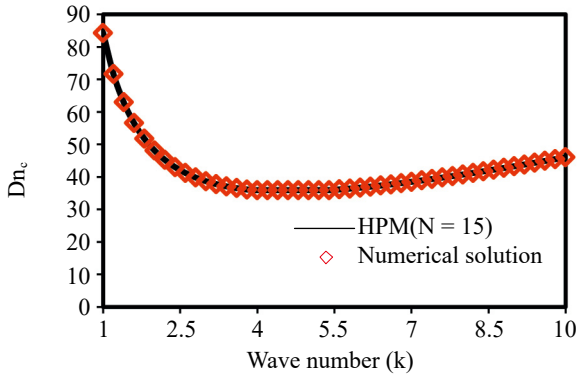


Fig. 3 Eigenvalue parameter of Dn_c under different k

truncated terms (N) is large enough that provides the solution with convergence criteria. Indeed, $e = \left| \left(Dn_c(N) - Dn_c(N-1) \right) . \left(Dn_c(N) \right)^{-1} \right| < 10^{-5}$, where $Dn_c(N)$ is the value of Dn_c calculated by semi-analytical method using 'N' number of truncated terms.

As shown in Fig. 3, the minimum Dean number is found 35.927 at k=3.952 by the HPM. Table 2 is given this critical Dean value by present study and other researchers [2, 16, 17, 22]. As indicated in Table 2, good accordance is visible between the results of HPM with available data of Dn_c and one can be concluded that the existing method of HPM has major applicability and effectiveness to study of eigenvalue problems such as linear hydrodynamic stability analysis.

4.2. Critical eigenvalue

By using a parametric analysis, linear hydrodynamic stability of fluid flow through the curved duct under the wide range of curvature ratios and aspect ratios is comprehensibly investigated. The considered cases and number of truncated terms used in HPM based on the convergence are tabulated in Table 3. As can be seen in Table 3, curvature ratios ranging from very small value of 0.01 to high value of 0.8 are considered under the aspect ratios from high value of 0.05 to small value of 1 (i.e., in x-direction which is in direction of curvature radius) and then from 1 to high value of 20 (i.e., in y-direction which is perpendicular to the direction of curvature radius).

Eigenvalues of critical complex wave number under different curvature ratios and aspect ratios are tabulated in Table 4. According to Table 4, the real parts of the eigenvalues of the critical wave numbers (k_r) have positive values, as expected. Furthermore, bifurcation with two branches of linearly stable mode (k_i^+) and linearly unstable mode (k_i^-) are visible for imaginary part of the eigenvalues of the critical wave numbers.

4.3. Effects of curvature ratio

In this section, as can be seen in Fig.4, the effects of curvature ratio on the onset of Dean instability under various aspect ratios are evaluated. According to Fig.4, for aspect ratios below the value of 1, the rate of the variation of Dn_c has very slight trend due to the increase in the curvature ratios. In addition, the more curvature ratio increases, the more Dn_c is monotonically increased (i.e., stabilizing effects), especially for larger tested aspect ratios. Therefore, as can be seen in this figure, larger curvature ratios have stabilizing effects. The reason behind this fact may be due to the significant effects of curvature ratios on the centrifugal forces that lead to the secondary flow motion in the curved ducts. Indeed, smaller curvature ratios amplify this phenomenon to the point that the motion of secondary flow will be intense. Accordingly, a decrease in the curvature ratios leads to hydrodynamic instability at the lower flow rates. In addition, higher flow rates (i.e., greater stream-wise velocities) is necessary to induce the fluid flow reversal through the curved rectangular ducts with higher curvature ratios and so, larger Dn_c are found for larger curvature ratios. This trend is also shown in experimental and numerical study of Fellouah et al. [6] and Sugiyama et al. [12], especially for curvature ratios ranging from 0.1 to 0.45.

Based on Fig.4 (b), it can be concluded that, for higher aspect ratios, the Dn_c shows prominent peak by the increase in the curvature ratios. This may be related to the fact that for curved ducts with larger aspect ratios, pressure distribution is more diffused at the outer wall of the duct and therefore, greater stream-wise flow rate is needed to prevent flow reversal at the outer wall.

Moreover, as can be seen in Fig.4, our Dn_c have higher or lower values compared to the archival data in some cases. Experimental results achieved from Sugiyama et al. [12] indicated a very small difference in Dn_c with the same aspect ratios with our results. Moreover, a little discrepancy is detectable between the present results and Fellouah et al. [6].Reason of this discrepancy is due to the different approach of finding the Dn_c under experimental, numerical and semi-analytical techniques. Indeed, appearance of the Dean vortices is a common method in experimental test for finding the onset of instability. Therefore, the quality of the visualization tools in experimental tests (qualitative visual method) has a major role in finding an accurate Dn_c. As a result, in experimental test, the Dean vortices are detectable when they are sufficiently intensified. In numerical methods, the number of iso-value contour is impressive in finding an accurate Dn_c. So, different overestimated or underestimated Dn_c are reported in the archival numerical and experimental studies. It is also notable that, in semi-analytical methods, the simplification assumptions on the basic flow or approximation of the solution are impressive on the value of reported Dn_c. It should also be noted that, in some cases, different values for aspect ratios and curvature ratios are considered compared to the archival experimental and numerical data.

4.4 Effects of aspect ratio

The effects of different aspect ratios on the onset of

https://doi.org/10.1017/jmech.2019.5 Published online by Cambridge University Press

Table 4 Eigenvalues of critical complex wave number under different curvature ratio and aspect ratios.

Curvature ratio (δ)	Aspect ratio (l)	Critical wave numbers	
		k_r	k_i
0.01	0.05	2.8039E-04	±1.8951E+09
	0.1	2.6195E-04	± 4.6112E+09
	0.5	2.3271E-03	± 3.8943E+10
	1	6.3962E-01	± 6.3009E+07
	5	2.0777E-04	± 6.5012E+11
	10	7.4649E+04	± 3.4546E+10
	20	1.9703E+05	± 9.1166E+10
0.05	0.05	6.2639E-05	± 3.0852E+08
	0.1	2.3454E-04	± 8.5199E+07
	0.5	2.1148E-02	± 4.2064E+11
	1	3.1696E-01	± 1.3596E+12
	5	1.5870E+00	± 6.8078E+12
	10	7.8442E+02	± 9.8161E+09
	20	1.3890E+01	± 5.9568E+13
0.1	0.05	1.0398E-03	± 8.3679E+08
	0.1	1.2740E-03	± 1.9922E+09
	0.5	1.5697E-02	± 1.7264E+10
	1	1.1144E-01	± 3.5235E+12
	5	5.7032E-01	± 1.8034E+13
	10	2.1509E+01	± 9.0990E+11
	20	4.9380E+00	± 1.5627E+14
0.2	0.05	2.7905E-04	± 3.2155E+06
	0.1	1.5427E-04	± 7.5631E+06
	0.5	4.0942E-02	± 3.2653E+07
	1	2.8332E-01	± 2.2906E+10
	5	1.3854E+00	± 1.1127E+11
	10	4.3867E-03	± 2.1634E+14
	20	9.0853E-03	± 4.4809E+14
0.4	0.05	2.1593E-01	± 7.0048E+07
	0.1	1.0314E-01	± 1.0045E+12
	0.5	1.2465E+00	± 8.6285E+12
	1	2.9158E-05	± 2.8007E+13
	5	1.4129E-04	± 1.3349E+14
	10	1.0183E+01	± 6.8521E+12
	20	1.8447E+01	± 1.2460E+13
0.6	0.05	3.9717E-02	± 1.1905E+10
	0.1	6.5849E-01	± 1.8417E+12
	0.5	1.5752E-01	± 2.7989E+10
	1	1.4525E-19	± 3.7268E+06
	5	1.5325E-21	± 3.9626E+07
	10	2.2212E-20	± 1.1436E+08
	20	2.6836E-18	± 9.0610E+07
0.8	0.05	3.5259E-06	± 6.3811E+06
	0.1	8.1876E-09	± 5.4439E+05
	0.5	9.1963E-08	± 3.4169E+06
	1	1.2926E-12	± 9.3613E+05
	5	5.2694E-13	± 2.8926E+08
	10	1.0877E-17	± 8.3492E+08
	20	1.3454E-17	± 1.4277E+09

https://doi.org/10.1017/jmech.2019.5 Published online by Cambridge University Press

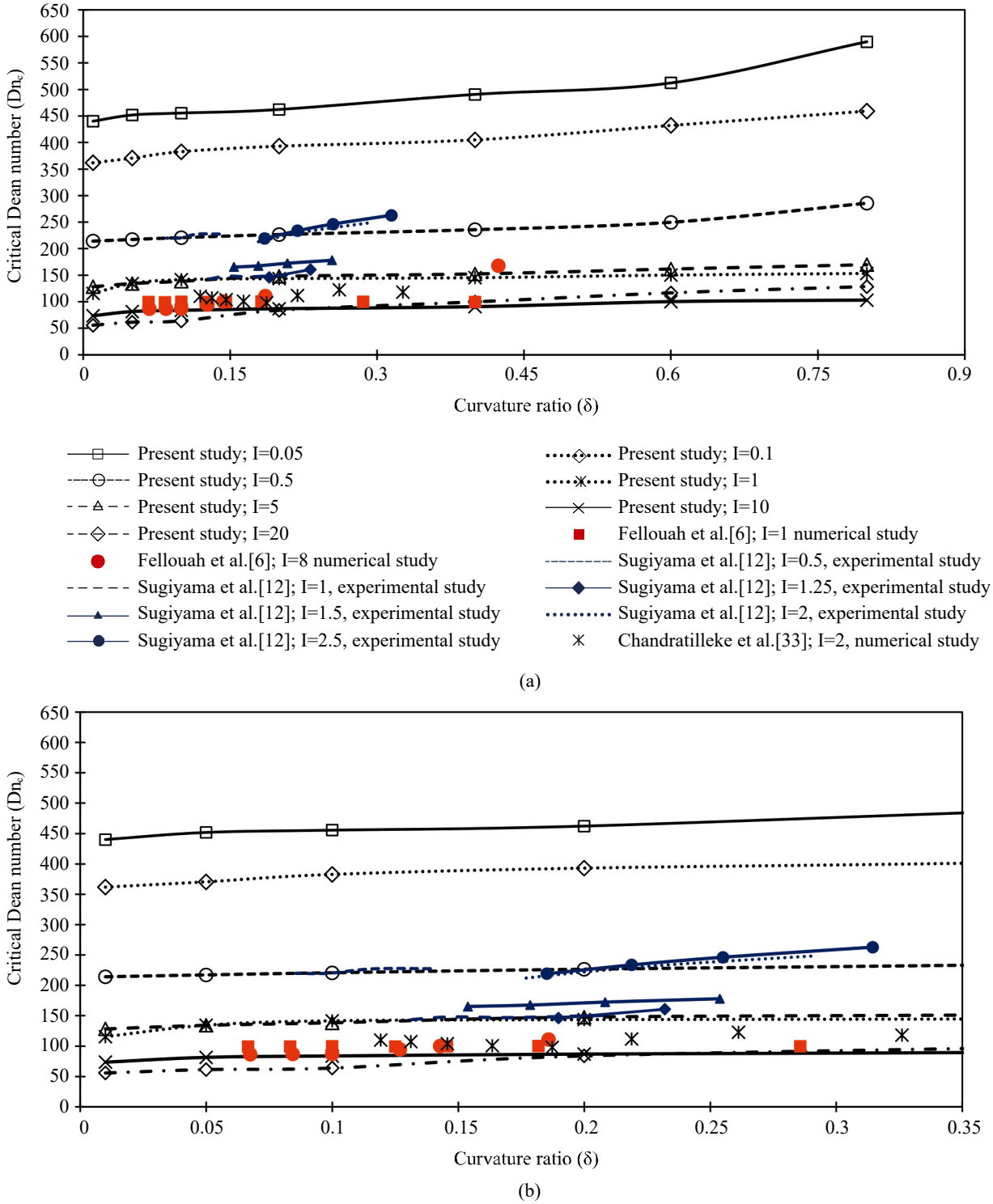


Fig. 4 Effects of curvature ratio on the onset of Dean instability (a) under different aspect ratios compared to archival data Refs. [6, 12, 33], (b) Enlarged diagram.

Dean instability is illustrated in Fig.5. As can be seen in Fig.5, the changes made to Dn_c under different aspect ratios have same trend at various tested curvature ratios. Regarding to the results, the Dn_c initially decreases as the duct aspect ratio increased from 0.5 to 1. Then, Dn_c is enhanced by an increase in the aspect ratio from 1 to about 5 and it is uniformly decreased again for aspect ratios ranging from 5 to 20. It is notable that, for l=5 to l=20, the rate of critical Dean growth by an increase in the aspect ratios is very low and we have approximately a fixed value in range of l=5 up to l=20. These trends show an appropriate accordance with the reported experimental and numerical studies in Ref. [4, 6, 12]. As mentioned above, due to discrepancies in measurement or computation methods, our reported Dn_c have insignificant lower or higher values compared to the archival data. The

https://doi.org/10.1017/jmech.2019.5 Published online by Cambridge University Press

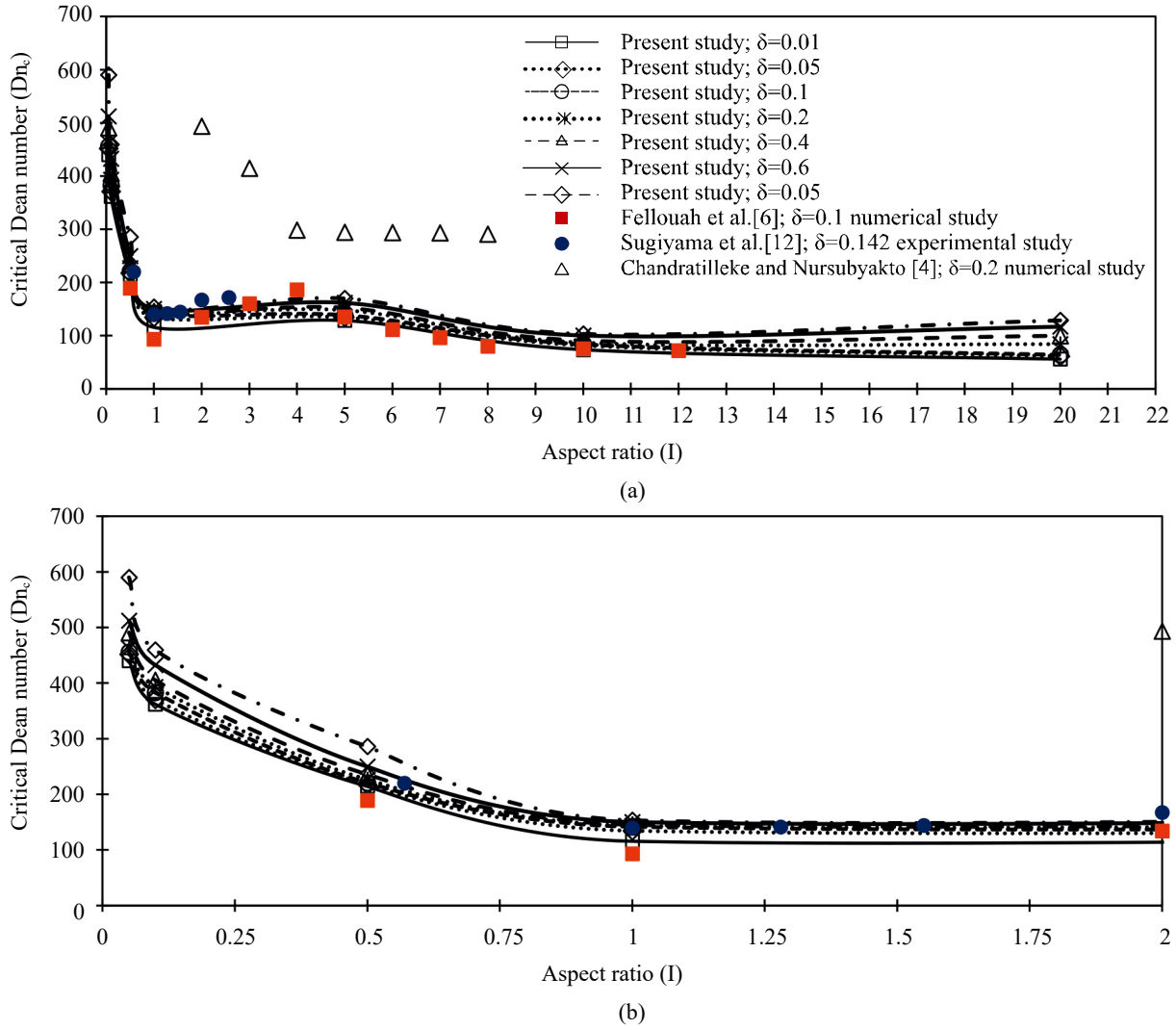


Fig. 5 Effects of aspect ratio on the onset of Dean instability (a) under different curvature ratios compared to archival data Ref. [4, 6, 12], (b) Enlarged diagram.

change of Dn_c according to the aspect ratio is significantly irregular, compared to the effects of curvature ratios. In addition, as can be seen in Fig. 5 (a) and (b), the change of Dn_c has significantly greater trend for the increase in the aspect ratios ranging from 0.05 to 1 (i.e., in x-direction which is in the direction of the curvature radius) compared to enhancement of aspect ratios ranging from 1 to 20 (i.e., in y-direction which is perpendicular to the direction of curvature radius). Therefore, one can conclude that, in order to obtain a greater reduction in Dn_c, the increase of aspect ratios may be applied in the direction of the curvature radius.

On the other hand, the irregular trend of Dn_c under different aspect ratios from phenomenological aspect may be related to the relative impression of secondary flow strength and the influences of confinement (i.e., space of Dean vortices to expand). Indeed, a decrease in the aspect ratio leads to more intense secondary flow and will result in destabilizing effects by decrease of the Dn_c. However, decrease of the aspect ratio causes an increase in the confinement effects which in turn results in stabilizing effects. Therefore, one can conclude that, for aspect ratios in range of 0.5 to 1,confinement effects is governed on fluid, while for l=1 to about l=5, secondary flow strength is dominant and for l>5, confinement effects is more impressive on instability of fluid flow again. Consequently, an increase in aspect ratios ranging from 0.5 to 1 has destabilizing effect. However, enhancement of aspect ratios from 1 to about 5 has stabilizing effects and an increase in aspect ratio larger than 5 has destabilizing effects on hydrodynamic stability of fluid flow in the curved ducts. It is also notable that, due to simultaneous effects of duct curvature (i.e., pressure driven) and energy gradient variations in cross stream of fluid flow through the curved ducts, the co-existence of secondary flow of first and second types is detectable in curved rectangular ducts [34, 35].

It is also notable that, according to Prandtl study [36], there are two different kinds of steady secondary motions in fluid flow. First kind (i.e., skew induced stream-wise vorticity) is initiated from mean flow related to the curvature effect (i.e., pressure driven) and second kind is originated by turbulence (i.e. turbulence driven) in transverse plane perpendicular to the stream-wise flow.

https://doi.org/10.1017/jmech.2019.5 Published online by Cambridge University Press

When the aspect ratios increase in the direction of the duct's curvature, the flow becomes more unstable that may be related to the increase the imbalance between the cross sectional Reynolds stress and stream-wise flow. While reduction of this imbalance is expected to be the reason of more stable flow (i.e. decrease of the possibility of secondary flow of Prandtl's second kind generation [36]) by increase of the aspect ratio perpendicular to the direction of curvature radius. So, irregular variation on Dn_c is achieved by increase of the aspect ratio according to described physical mechanisms.

It should be noted that, Winters [3], Yanase et al. [5], and Yanase et al. [37] indicted that the symmetry assumption of basic flow and disturbances are only valid for one and two-vortex secondary flows and solution with these symmetry assumptions are unable to predict the secondary flow with four and more-vortexes. Thus, as may be found in literature, Yanase et al. [5] investigated instability in curved rectangular duct for $Dn_c<670$, where new bifurcation is appeared under symmetric solution for $Dn_c>670$ in case of square duct. Winters [3] also indicated the validity of symmetry flow assumption only up to $Dn_c<680$, where he showed the change of secondary flow pattern from two-vortex to four-vortex for square duct at Dn_c greater than 680. On the other hand, in experimental study, Cheng and Mok [38] found the onset of four-vortex secondary flow for $Dn_c>1710$. Sugiyama et al. [12] also observed four-vortex pattern on secondary flow for $Dn_c>570$ for square curved duct with curvature ratio $\delta=0.125$.

According to above description, one may be concluded that, present results of the Dn_{cs} are reliable for prediction of hydrodynamic instability under symmetry flow assumption. This is may be due to the linear hydrodynamic stability analysis that the Dn_c is corresponding to the points of bifurcation (which are proportional to formation of Dean vortices). Also, the present results of Dn_{cs} under tested aspect ratios and curvature ratios have lower values compare to other reported Dn_c in Refs [3, 5, 12, 37, 38] which are corresponding to four-vortex secondary flow generation. Therefore, the symmetry flow assumption is valid in our tested conditions. However, to specify the maximum limitation of Dn_{cs} under symmetry condition, it is necessary to conduct experimental studies to determine the Dn_{cs} proportional to formation of four-vortex secondary flow in the realistic cases.

5. CONCLUSIONS

A semi-analytical technique of HPM is successfully applied on eigenvalue problem arising from linear hydrodynamics stability. It is developed for symmetric disturbances of fluid flow through the curved rectangular duct under different curvature ratios ranging from 0.01 to 0.8 and aspect ratios in range of 0.05 to 20. The semi-analytical results are compared and validated by experimental data and other numerical solutions in the literature with good accuracy. Among the most important extracted findings in this study, the following conclusions may be drawn:

(1) For all the intended aspect ratios, when the curvature ratio is increased the flow becomes more stable by increasing of the Dn_c. By increasing in curvature ratio, the Dn_c growth rate is more visible for aspect ratios ranging from 0.05 to 1.

(2) Irregular behavior on variation of Dn_c is observed by an increase in the aspect ratio under different curvature ratios. We found that, as the aspect ratios increases in the direction of curvature radius, i.e., from 0.05 to 1, fluid flow becomes unstable by reduction of the Dn_c. While, as the aspect ratio increases from 1 to about 5, Dn_c is increased and fluid flow becomes stable. In addition, for aspect ratios larger than 5 to 20, the rate of the variations of Dn_c is insignificant and the Dn_c is lightly decreased.

(3) The Dn_c and corresponding eigenvalues of critical complex wave number are calculated and reported at different curvature ratios and aspect ratios.

The current paper deserves further study in the future. Evaluation of other semi-analytical techniques such as HAM, VIM, ADAM and FTADM is proposed for more investigation on the linear hydrodynamic stability of fluid flow through the curved ducts. In addition, the study on Dn_{cs} for onset of instability of flow in curved rectangular ducts under different externalities, i.e., temperature, electrical and magnetic fields can be considered in future works.

REFERENCES

1. Fischer, A.C., Forsberg, F., Lapisa, M., Bleiker, S.J., Stemme, G., Roxhed, N. and Niklaus, F., "Integrating MEMS and ICs," *Microsystems & Nanoengineering*, **1**, pp.1–16 (2015).
2. Drazin, P.G. and Reid, W.H., *Hydrodynamic Stability*, 2nd Edition, Cambridge University Press, Cambridge (2004).
3. Winters, K.H., "A Bifurcation Study of Laminar Flow in a Curved Tube of Rectangular Cross-Section," *Journal of Fluid Mechanics*, **180**, pp.343–369 (1987).
4. Chandratilleke, T.T. and Nursubyakto, A.,"Numerical Prediction of Secondary Flow and Convective Heat Transfer in Externally Heated Curved Rectangular Ducts," *International Journal of Thermal Sciences*, **42**, pp.187–198 (2003).
5. Yanase, S., Kaga, Y. and Daikai, R., "Laminar Flows through a Curved Rectangular Duct over a Wide Range of the Aspect Ratio," *Fluid Dynamics Research*, **31**, pp.151–183 (2002).
6. Fellouah, H., Castelain, C., El Moctar, A.O. and Peerhossaini, H., "A Criterion for Detection of the Onset of Dean Instability in Newtonian Fluids," *European Journal of Mechanics-B/Fluids*, **25**, pp.505–531 (2006).
7. Boutabaa, M., Helin, L., Mompean, G. and Thais,

https://doi.org/10.1017/jmech.2019.5 Published online by Cambridge University Press

L.,"Numerical Study of Dean Vortices in Developing Newtonian and Viscoelastic Flows through a Curved Duct of Square Cross-Section," *Comptes Rendus Mecanique*, **337**, pp.40–47 (2009).

8. Vinuesa, R., Noorani, A., Lozano-Durán, A., Khoury, G.K.E., Schlatter, P., Fischer, P.F. and Nagib, H.M., "Aspect Ratio Effects in Turbulent Duct Flows Studied through Direct Numerical Simulation," *Journal of Turbulence*, **15**, pp.677–706 (2014).
9. Tanveer, A., Hayat, T., Alsaedi, A. and Ahmad, B., "Heat Transfer Analysis for Peristalsis of MHD Carreau Fluid in a Curved Channel through Modified Darcy Law," *Journal of Mechanics*, pp. 1–9 (2018).
10. Ligrani, P.M. and Niver, R.D., "Flow Visualization of Dean Vortices in a Curved Channel with 40 to 1 Aspect Ratio," *The Physics of Fluids*, **31**, pp.3605–3617 (1988).
11. Yamamoto, K., Wu, X., Nozaki, K. and Hayamizu, Y., "Visualization of Taylor–Dean Flow in a Curved Duct of Square Cross-Section," *Fluid Dynamics Research*, **38**, pp.1–18 (2006).
12. Sugiyama, S., Hayashi, T. and Yamazaki, K., "Flow Characteristics in the Curved Rectangular Channels: Visualization of Secondary Flow," *Bulletin of JSME*, **26**, pp.964–969 (1983).
13. Dean, W.R., "Fluid Motion in a Curved Channel," *Proceedings of the Royal Society of London, Series A*, **121**, pp. 402–420 (1928)
14. Topakoglu, H.C., "Steady Laminar Flow of an Incompressible Viscous Fluid in a *Curved Pipe," Journal of Mathematics and Mechanics*, **16**, pp.1231–1237 (1967).
15. Finlay, W.H. and Nandakumar, K., "Onset of Two-Dimensional Cellular Flow in Finite Curved Channels of Large Aspect Ratio," *Physics of Fluids A: Fluid Dynamics*, **2**, pp.1163–1174 (1990).
16. Walowit, J., Tsao, S. and Diprima, R.C., "Stability of Flow between Arbitrarily Spaced Concentric Cylindrical Surfaces Including the Effect of a Radial Temperature Gradient," *Journal of Applied Mechanics*, **31**, pp.585–593 (1964).
17. Deka, R.K. and Takhar, H.S., "Hydrodynamic Stability of Viscous Flow between Curved Porous Channel with Radial Flow," *International Journal of Engineering Science*, **42**, pp.953–966 (2004).
18. Chen, K.T., Yarn, K.F., Chen, H.Y., Tsai, C.C., Luo, W.J. and Chen, C.N., "Aspect Ratio Effect on Laminar Flow Bifurcations in a Curved Rectangular Tube Driven by Pressure Gradients," *Journal of Mechanics*, **33**, pp.831-840 (2017).
19. Orszag, S.A., "Accurate Solution of the Orr–Sommerfeld Stability Equation," *Journal of Fluid Mechanics*, **50**, pp.689–703 (1971).
20. Yamamoto, K., Yanase, S. and Jiang, R., "Stability of the Flow in a Helical Tube," *Fluid Dynamics Research*, **22**, pp.153–170 (1998).
21. Mondal, R.N., Islam, M.Z., Islam, M.M. and Yanase, S., "Numerical Study of Unsteady Heat and Fluid Flow through a Curved Rectangular Duct of Small Aspect Ratio," *Thammasat International Journal of Science and Technology*, **20**, pp.1–20 (2015).
22. Deka, R.K. and Paul, A., "Stability of Taylor–Couette and Dean Flow: A Semi-analytical Study," *Applied Mathematical Modelling*, **37**, pp.1627–1637 (2013).
23. He, J.H., "A Review on Some New Recently Developed Nonlinear Analytical Techniques," *International Journal of Nonlinear Sciences and Numerical Simulation*, **1**, pp.51–70 (2000).
24. Batchelor, G.K., *An Introduction to Fluid Dynamics*, 1st Edition, Cambridge University Press, Cambridge (2000).
25. Hille, P., Vehrenkamp, R. and Schulz-Dubois, E.O., "The Development and Structure of Primary and Secondary Flow in a Curved Square Duct," *Journal of Fluid Mechanics*, **151**, pp. 219–241 (1985).
26. Mees, P.A., Nandakumar, K. and Masliyah, J.H., "Secondary Instability of Flow in a Curved Duct of Square Cross-Section," *Journal of Fluid Mechanics*, **323**, pp. 387–409 (1996).
27. Huerre, P. and Monkewitz, P.A., "Local and Global Instabilities in Spatially Developing Flows," *Annual Review of Fluid Mechanics*, **22**, pp.473–537 (1990).
28. Mahapatra, T.R., Dholey, S. and Gupta, A.S., "Stability of Hydromagnetic Dean Flow between Two Arbitrarily Spaced Concentric Circular Cylinders in the Presence of a Uniform Axial Magnetic Field," *Physics Letters A*, **373**, pp.4338–4345 (2009).
29. Bottaro, A., "Spatially Developing Flow in Curved Duct," *Numerical Methods in Laminar and Turbulent Flow*, **7**, pp. 696–706 (1991).
30. Chomaz, J.M., "Absolute and Convective Instabilities in Nonlinear Systems," *Physical Review Letters*, **69**, pp.1931–1934 (1992).
31. Bottaro, A., "On Longitudinal Vortices in Curved Channel Flow," *Journal of Fluid Mechanics*, **251**, pp.627–660 (1993).
32. Maple, Maple User Manual, Version 18.02, *The Waterloo Maple Inc* (2014).
33. Chandratilleke, T., Nadim, N. and Narayanaswamy, R., "Analysis of Secondary Flow Characteristics and Hydrodynamic Instability in Fluid Flow through Curved Ducts," *Proceedings of the 8th International Conference on Heat Transfer, Fluid Mechanics and Thermodynamics*, Mauritius (2011).
34. Vidal, A., Vinuesa, R., Schlatter, P. and Nagib, H.M., "Influence of Corner Geometry on the Secondary Flow in Turbulent Square Ducts," *International*

https://doi.org/10.1017/jmech.2019.5 Published online by Cambridge University Press

Journal of Heat and Fluid Flow, **67**, pp.69–78 (2017).

35. Nowruzi, H., Ghassemi, H. and Nourazar, S.S., "On Hydrodynamic Stability of Dean Flow by Using Energy Gradient Methods," *Journal of Mechanics*, pp.1–14 (2018).
36. Prandtl, L., Essentials of Fluid Dynamics: With Applications to Hydraulics, Aeronautics, Meteorology and Other Subjects, 1st Edition, Hafner Publishing Company, New York (1952).
37. Yanase, S., Goto, N. and Yamamoto, K., "Dual Solutions of the Flow through a Curved Tube," *Fluid Dynamics Research*, **5**, pp.191–201 (1989).
38. Cheng, K.C. and Mok, S.Y., "Flow Visualization Studies on Secondary Flow Patterns and Centrifugal Instability Phenomena in Curved Tubes," *Fluid Control and Measurement*, **2**, pp.765–773 (1986).

(Manuscript received October 11, 2018,
accepted for publication January 14, 2019.)

https://doi.org/10.1017/jmech.2019.5 Published online by Cambridge University Press